doi:10.1038/nature10416

Electrons surfing on a sound wave as a platform for quantum optics with flying electrons

Sylvain Hermelin[1], Shintaro Takada[2], Michihisa Yamamoto[2,3], Seigo Tarucha[2,4], Andreas D. Wieck[5], Laurent Saminadayar[1,6], Christopher Bäuerle[1] & Tristan Meunier[1]

Electrons in a metal are indistinguishable particles that interact strongly with other electrons and their environment. Isolating and detecting a single flying electron after propagation, in a similar manner to quantum optics experiments with single photons[1,2], is therefore a challenging task. So far only a few experiments have been performed in a high-mobility two-dimensional electron gas in which the electron propagates almost ballistically[3–5]. In these previous works, flying electrons were detected by means of the current generated by an ensemble of electrons, and electron correlations were encrypted in the current noise. Here we demonstrate the experimental realization of high-efficiency single-electron source and detector for a single electron propagating isolated from the other electrons through a one-dimensional channel. The moving potential is excited by a surface acoustic wave, which carries the single electron along the one-dimensional channel at a speed of 3 μm ns^{-1}. When this quantum channel is placed between two quantum dots several micrometres apart, a single electron can be transported from one quantum dot to the other with quantum efficiencies of emission and detection of 96% and 92%, respectively. Furthermore, the transfer of the electron can be triggered on a timescale shorter than the coherence time T_2* of GaAs spin qubits[6]. Our work opens new avenues with which to study the teleportation of a single electron spin and the distant interaction between spatially separated qubits in a condensed-matter system.

Quantum electron optics is a field aiming at the realization of photon experiments with flying electrons in nanostructures at the single-electron level. Important tools with which to infer complex photon correlations inaccessible from ensemble measurements are single-photon sources and single-photon detectors. In contrast with photons, electrons are strongly interacting particles and they usually propagate in a Fermi sea filled with other electrons. Each electron therefore inevitably mixes with the others of the Fermi sea, which implies that the quantum information stored within the charge or the spin of the single electron will be lost over short lengths. To perform quantum electron-optical experiments at the single-electron level, one therefore needs a source of single electrons, a controlled propagating medium and a single-electron detector. It has been proposed that edge states in the quantum Hall effect can serve as a one-dimensional (1D) propagating channel for flying electrons. As a result of Coulomb blockade, quantum dots have been demonstrated to be a good source of single electrons[7,8] and can also serve as a single-electron detector. Indeed, once an electron has been stored in a quantum dot, its presence can be inferred routinely by charge detection[9]. Nevertheless, re-trapping the electron in another quantum dot after propagation in an edge state turns out to be extremely difficult, and currently all the information extracted from such experiments is coming from ensemble measurements[10,11]. Here we show that a single flying electron—an electron surfing on a sound wave—can be sent on demand from a quantum dot by means of a 1D quantum channel and re-trapped in a second quantum dot after propagation. The 1D quantum channel consists of a depleted region several micrometres long in a two-dimensional electron gas (2DEG). The electron is dragged along by exciting a surface acoustic wave (SAW) and propagates isolated from the other electrons inside the 1D channel[12]. The processes of loading and unloading of the flying electron from the quantum channel into a quantum dot turn out to be highly efficient. Moreover, we show that the transfer of the electron can be triggered with a timescale smaller than the coherence time T_2* of GaAs spin qubits[6]. Because both electron spin directions are treated on the same foot in the SAW quantum channel, one expects that the spin coherence during the transport is conserved. Naturally, new possibilities will emerge to address the question of scalability in spin qubit systems[6,13,14].

To transport a single electron from one quantum dot to the other separated by a 3-μm 1D channel (see Fig. 1 and Methods), the following procedure is applied. First, the region between the two electrodes, which define the 1D channel, is fully depleted. As a consequence, direct linear electron transport from one end of the channel to the other is blocked because the Fermi energy lies below the potential induced by the gates. Second, by applying microwave excitation to the interdigitated transducer (IDT), SAW-induced moving quantum dots are generated[12] as a result of the piezoelectric properties of GaAs (see also Supplementary Information). By adding a quantum dot to each side of the 1D channel and tuning both quantum dots into the single electron regime, it is then possible to transport a single electron from one quantum dot across the 1D channel and catch it inside the second quantum dot. Stability diagrams for both quantum dots as a function

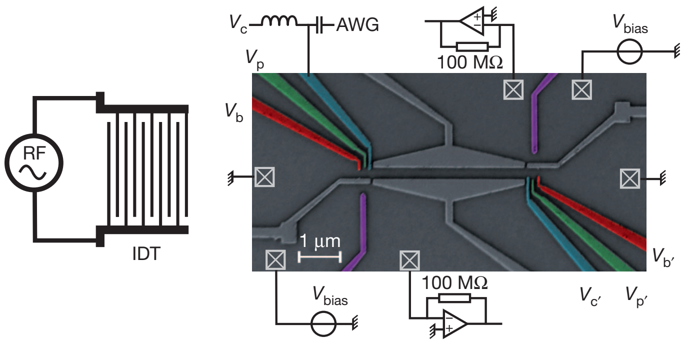

Figure 1 | Experimental device and measurement setup. Scanning electron microscope image of the single-electron transfer device, and diagram of the experimental setup. Two quantum dots, which can be brought into the single-electron regime, are separated by a 1D channel 3 μm long, as shown. Each quantum dot is capacitively coupled to a QPC close by that is used as an electrometer[9]. By applying a microwave burst 65 ns long on the IDT (see Methods for details), a train of about 150 moving quantum dots is created in the 1D channel. Gate V_c is connected to a home-made bias tee to allow nanosecond manipulation of the dot potential. RF, radio frequency.

[1]Institut Néel, CNRS, and Université Joseph Fourier, 38042 Grenoble, France. [2]Department of Applied Physics, University of Tokyo, Tokyo, 113-8656, Japan. [3]ERATO-JST, Kawaguchi-shi, Saitama 331-0012, Japan. [4]ICORP (International Cooperative Research Project) Quantum Spin Information Project, Atsugi-shi, Kanagawa, 243-0198, Japan. [5]Lehrstuhl für Angewandte Festkörperphysik, Ruhr-Universität Bochum, Universitätsstrasse 150, 44780 Bochum, Germany. [6]Institut Universitaire de France, 103 boulevard Saint-Michel, 75005 Paris, France.

of the applied voltage on the two gates controlling the two barriers of the quantum dot are shown in Fig. 2a, b. They demonstrate that the system can be tuned into a regime consisting of few electrons[15]. As expected, the charge degeneracy lines disappear when the barrier height between each dot and the reservoir is increased (corresponding to increasingly negative voltages V_b and $V_{b'}$). This also changes the position of the quantum-dot minimum and brings the electron closer to the 1D channel, to a position where a better transfer to SAW quantum dots is expected.

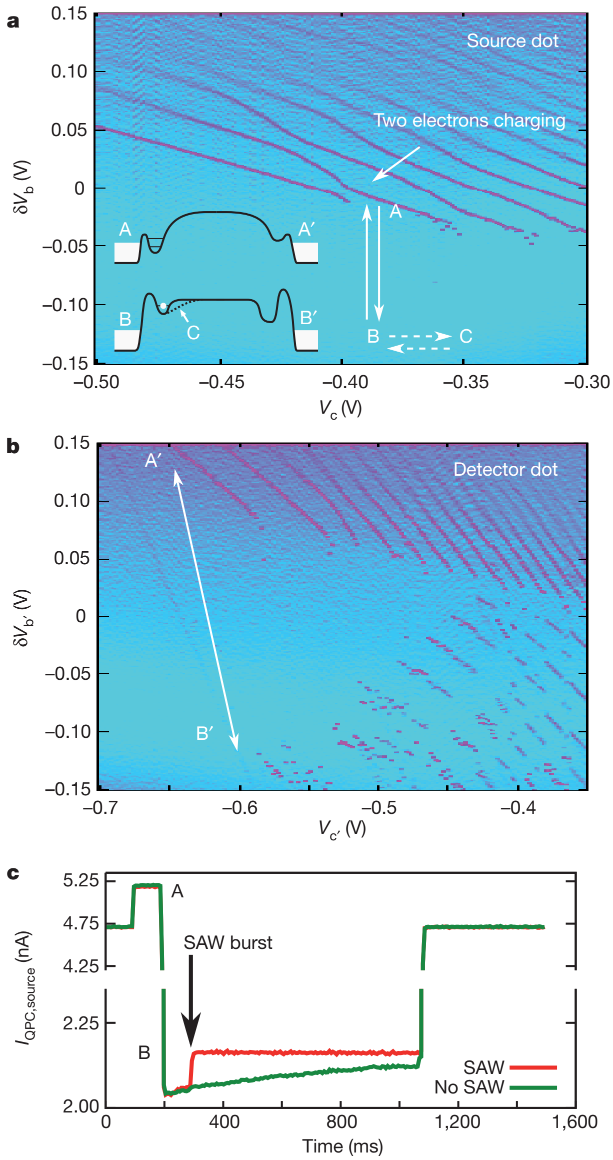

Figure 2 | Stability diagrams of the two quantum dots and charge detection. **a**, **b**, Stability diagram of the left (**a**) and right (**b**) dot obtained via charge detection by varying respectively gate voltages (V_b or V_c) and ($V_{b'}$ or $V_{c'}$) (see Fig. 1). Sweeps in V_b and $V_{b'}$ are fast and are performed within 1 s from +0.15 V to −0.15 V (3 ms per point). When the barrier height is made higher (V_b or $V_{b'}$ more negative), metastable charge states with timescales longer than the V_b or $V_{b'}$ sweep time are observed. In the very negative $V_{b'}$ part of the diagram for the right dot, the electrons will finally tunnel out. When the sweep direction of $V_{b'}$ is reversed, these charge detection steps are absent. Inset to **a**: schematic diagram of the dots and channel electrostatic potential applied by the gates to the electron at different points in the stability diagram (see the text). **c**, Average QPC time trace along the voltage sequence of the single-electron source. Without the microwave burst applied on the IDT, we observe a lifetime for the metastable one-electron charge state of 700 ms. Applying a microwave burst, the electron in the metastable state is forced to quit the quantum dot with very high probability.

The protocol of the single-electron source for a SAW quantum channel is a sequence made of three dot-gate voltage steps (see Fig. 2a). At working point A on Fig. 2a, the left quantum dot (the single-electron source) is loaded with one electron on a timescale close to microseconds and unresolved with the setup detection bandwidth. It is then brought rapidly to working point B, where the chemical potential of the single electron state lies above the Fermi energy and the coupling to the 1D channel is expected to be large. The actual position of B is not crucial as long as the electron is sufficiently protected from tunnelling out of the dot and the dot potential is high enough to facilitate the charging of the electron into the moving SAW dot (see inset to Fig. 2a). For each sequence, the quantum point contact (QPC) conductance time-trace is recorded to observe single-shot loading and unloading of the dot. This sequence is repeated 1,000 times to obtain measurement statistics; the resulting averaged time-traces are shown in Fig. 2c. An exponential decay of the presence of the electron in the dot as a function of the time spent at working point B is observed in the experimental data, corresponding to a tunnelling time close to 1 s as indicated by the green line. This gate pulsing sequence is then repeated by adding a burst of microwaves to the IDT with a pulse length of several tens of nanoseconds, applied 100 ms after the system is brought into position B. The microwave burst creates a moving quantum dot, which lifts the electron, initially trapped in the left quantum dot, above the tunnel barrier and drags it out of the quantum dot. This results in a jump in the QPC current, as shown by the red line.

To demonstrate that the electron has been loaded into a moving quantum dot and not expelled into the reservoir, it is essential to detect the coincidence between events when the electron leaves the single-electron source (left dot) and when it is trapped in the single-electron detector (right dot). This is realized by a second voltage pulse sequence on the right dot: when the single-electron source is brought in position B, the detector dot is armed by pulsing its gates to working point B′, where the steady state is the zero-electron state and the coupling to the channel is large. At this working point both QPC traces are recorded simultaneously. No charge variation is observed during the first 50 ms where the system is kept in position B. A microwave pulse is sent with a time lag of 50 ms. After the recording, the detector is reinitialized to zero electron at working point A′, where the captured electron can tunnel efficiently into the reservoir. Typical single-shot readout curves are presented in Fig. 3a–d. Coincidences are observed between events when an electron leaves the source quantum dot and an electron is detected in the receiver quantum dot within the same time slot (Fig. 3a). These events correspond to the situation in which one electron has been loaded in the electron source (left dot), is then transferred in the quantum channel (the moving quantum dots) and is received in the detector (right dot). In contrast with photon detectors, here the electron still exists after detection. A set of experiments described in Fig. 3 allows the full characterization of the high quantum efficiency of both the single-electron source and the single-electron detector observed in the experiment: 96% for the single-electron source and 92% for the single-electron detector (see Fig. 3e).

In quantum dots it is possible to load not just one but two electrons. By waiting long enough[16], the two electrons will be in a singlet state at zero magnetic field and are hence entangled in the spin degree of freedom. The ability to separate the two electrons and to bring only one of them to the second quantum dot is of potential interest for the transfer of quantum information and is the essence of the quantum teleportation protocol[2,17–19]. By analogy with photons, this is the equivalence of a two-photon entangled source[20]. Moreover, in contrast with a photon detector, the electron detector can discriminate easily whether one, two or more electrons have left the single-electron source and are captured in the single-electron detector (see Fig. 2a). The protocol consists of loading the left dot with exactly two electrons by moving gate voltages V_b and V_c into the two-electron regime of the stability diagram. The quantum dot is then tuned towards the working point where loading of the moving quantum dots is possible (point B).

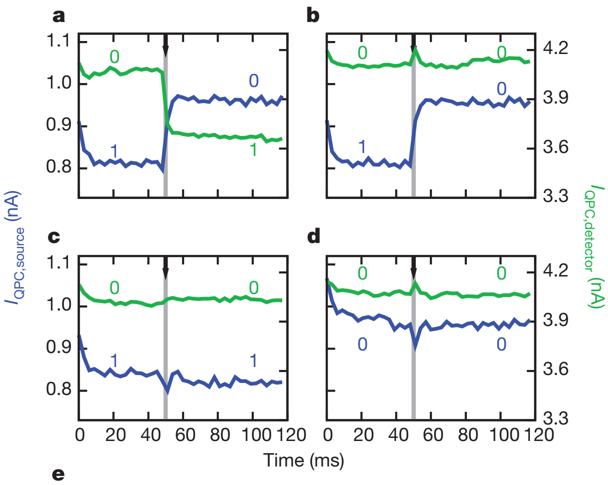

e

Event	SAW On	Off	On	On	On
N_{1xxx}	9,841	10,001	16	5,154	1,462
N_{10xx}	9,408 (95.6%)	0 (0%)	15 (94%)	4,954 (96.1%)	1,395 (95.4%)
N_{100x}	9,128	0	14	4,807	1,349
N_{1001}	8,393 (91.9%)	0 (0%)	14 (100%)	4,417 (91.9%)	1,244 (92.2%)
$\Sigma N_{\alpha\beta\gamma\delta}$	0	1	0	0	0

Figure 3 | Coincidence between emission and detection of a single electron. **a**–**d**, Coincidence between the two single-shot QPC time traces at voltage working points B and B′ corresponding to the different events N_{1001} (**a**), N_{1000} (**b**), N_{1100} (**c**) and N_{0000} (**d**). The position in time of the RF burst is indicated by the black arrow. At this specific time, the small peak or dip observed on time traces is the result of the SAW-induced enhancement or reduction, respectively, of the QPC current. The notation $N_{\alpha\beta\gamma\delta}$ corresponds to the number of events with α or β electrons in the source dot before or after the microwave burst, respectively, and to γ or δ electrons in the receiver dot before or after the microwave burst, respectively. When one index is replaced by x, the corresponding output result is disregarded. Event N_{1000} corresponds to the situation in which the electron has been transferred from the source to the detector and is immediately kicked out of the detector dot by the same RF burst and is therefore not detected. Events for which $\beta + \delta > \alpha + \gamma$ are called 'bad' events. **e**, Summary table for the different events over 10,001 traces for different source dot loading probabilities (N_{1xxx}) with or without the RF burst. The loading probability can be tuned on demand by changing the voltage gate position A in the stability diagram around the charge degeneracy point. The summation at the bottom table is for $(\beta + \alpha) > \delta + \gamma$.

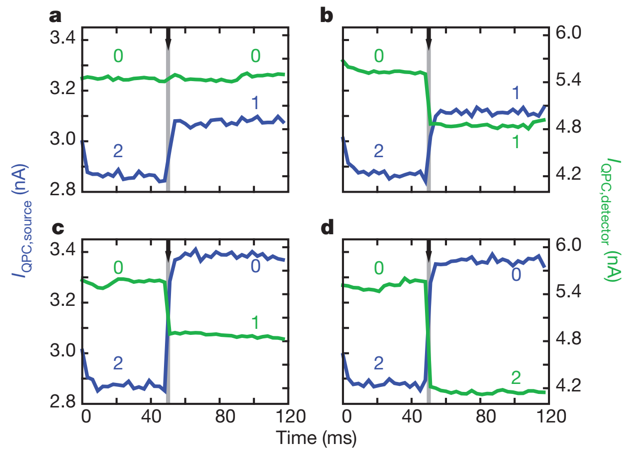

e

Event	V_c (mV) −388	−322
N_{21xx}	445 (44.3%)	970 (96.5%)
N_{2101}	443 (99.6%)	878 (90.5%)
N_{20xx}	558 (55.5%)	30 (3%)
N_{2001}	62 (11%)	4 (13%)
N_{2002}	496 (88.9%)	26 (87%)

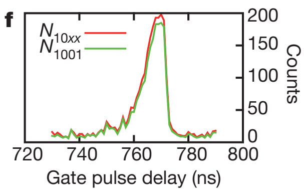

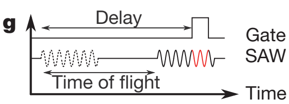

Figure 4 | Coincidence between emission and detection of two electrons and triggered nanosecond electron transfer. **a**–**d**, Coincidence between the two single-shot QPC time traces at voltage working points B and B′ corresponding to the different events N_{2100} (**a**), N_{2101} (**b**), N_{2001} (**c**) and N_{2002} (**d**). **e**, Summary table of the different events over 1,005 traces for dot configurations $V_c = -0.388$ V and $V_c = -0.322$ V. **f**, Evolution of the number of N_{1001} and N_{10xx} events as a function of the delay between the 1-ns gate pulse and the 65-ns microwave burst when a single electron is loaded into the single-electron source. **g**, Schematic diagram of the timing sequence between the 1-ns gate pulse and the microwave burst applied to the IDT.

Different possibilities for the emission of electrons into the quantum channel are observed. Indeed, when starting with exactly two electrons in the source dot, one can achieve the outcome that either exactly one or both electrons are emitted from the source and received in the detector dot, as shown by the single-shot traces for QPC detection of the two dots (see Fig. 4a–d). The probability of each event varies with the working voltage at point B. For very negative gate voltage V_c, about half of the time the two electrons are separated, meaning that only one electron is transferred, and the other half of the time both electrons are transported (see Fig. 4e). For the events in which both electrons leave the dot, the electrons are most probably loaded into two different moving quantum dots. More interestingly, when pulsing gate voltage V_c more positively, a situation can be realized in which only one of the two electrons of the left dot is efficiently emitted and consequently captured by the right dot (see Fig. 4e). In this case, the probability of sending the two electrons is markedly reduced, to less than 3%, and the probability of effectively separating the two electrons approaches 90%.

To use single-electron transfer in quantum operations using spin qubits, one has to show that coherence of the electron spin after electron transfer is preserved. Measurement and coherent manipulations of electron spins can be straightforwardly implemented in our setup, and the spin coherence time T_2^* of an ensemble of electrons stored in SAW-assisted moving quantum dots has been shown to be as long as 25 ns (ref. 21). A necessary condition for investigating coherent transport of a single electron spin is to be able to trigger the electron transfer within a timescale that is short compared with T_2^*. Indeed, a microwave pulse 250 ns in duration corresponds to about 700 moving quantum dots, and the experiments described above demonstrate the ability to load the electron into one of the moving quantum dots produced by each SAW microwave burst. We now show that the number of minima of the microwave burst in which the electron is loaded can be reduced to two. For this purpose, the single-electron source voltage sequence is slightly modified. After charging of the quantum dot, the system is brought to position B (see Fig. 2a) slightly on the more negative side with respect to V_c, and the duration of the microwave pulse is shortened to a minimum of 65 ns. At this voltage position, the barrier height to the quantum channel is increased and the transfer probability of an electron into the quantum channel is as low as 5% when excited with the SAW microwave burst. To trigger single-electron transfer, a 1-ns voltage pulse on V_c with a positive value (voltage position C in Fig. 2a) is added to this sequence. In Fig. 4f the evolution of the number of events in which one electron leaves the single-electron source and one electron is detected in the single-electron detector (N_{1001}) is plotted as a function of the delay between the 1-ns gate pulse and the 65-ns microwave burst. High transfer probabilities reaching 90% are observed only for time delays of roughly 765 ns, corresponding to the propagation time of the surface acoustic wave from the IDT to the dot region. Taking into account the pulse length of the gate and the distance between two minima of the SAW, only two moving quantum dots can then be the hosts of the transported electron during the gate pulse, as indicated schematically in Fig. 4g. This demonstrates the ability to load on demand and in a very reproducible manner one of the two minima of the train of moving quantum dots with a single electron during the 1-ns gate pulse. The use of a faster arbitrary waveform generator should allow the electron to be loaded on demand into the same moving quantum dot.

These experiments represent the first milestone on the road to a new experimental platform for realizing quantum optics with flying electrons implemented in gated 2DEG heterostructures and transported by surface acoustic waves. High quantum efficiency of both the single-electron detector and the single-electron source are shown and potentially enable the measurement of all moments of the electron correlations[22]. In comparison with other implementations in similar systems, the propagating electron is physically isolated from the other conduction electrons of the heterostructure. In bringing together two propagating quantum buses separated by a tunnel barrier, a beam splitter for flying electrons can be implemented[23,24] and Hanbury Brown and Twiss-type experiments in which there are stronger Coulomb interactions between electrons could be realized. Future experiments should allow coherent spin transfer and provide new insight into the feasibility of quantum teleportation protocols and on the potential scalability of spin qubits.

METHODS SUMMARY

The device is defined by Schottky gates in an n-AlGaAs/GaAs 2DEG-based heterostructure (the properties of the 2DEG are as follows: $\mu \approx 10^6\,\mathrm{cm^2\,V^{-1}\,s^{-1}}$, $n_s \approx 1.4 \times 10^{11}\,\mathrm{cm^{-2}}$, depth 90 nm) with standard split-gate techniques. The charge configuration of both dots is measured by means of the conductance of both QPCs by biasing it with a direct-current voltage of 300 μV; the current is measured with a current-to-voltage converter with a bandwidth of 1.4 kHz. The voltage on each gate can be varied on a timescale down to microseconds. In addition, the gate biased with voltage V_c, controlling the coupling between the left dot and the 1D channel, is connected to a homemade bias tee to allow nanosecond manipulation of the dot potential by means of an arbitrary function generator (Tektronix AWG 5014). The IDT, which is placed about 2 mm to the left of the sample, is made of 70 pairs of lines 70 μm in length and 250 nm in width with a 1-μm spacing. The IDT is orientated perpendicular to the direction of the 1D channel defined along the crystal axis [110] of the GaAs wafer; it has a frequency bandwidth of about 20 MHz.

Received 26 April; accepted 4 August 2011.

1. Aspect, A., Grangier, P. & Roger, G. Experimental tests of realistic local theories via Bell's theorem. *Phys. Rev. Lett.* **47,** 460–463 (1981).
2. Bouwmeester, D. *et al.* Experimental quantum teleportation. *Nature* **390,** 575–579 (1997).
3. Neder, I. *et al.* Interference between two indistinguishable electrons from independent sources. *Nature* **448,** 333–337 (2007).
4. Henny, M. *et al.* The fermionic Hanbury Brown and Twiss experiment. *Science* **284,** 296–298 (1999).
5. Liu, R. C., Odom, B., Yamamoto, Y. & Tarucha, S. Quantum interference in electron collision. *Nature* **391,** 263–265 (1998).
6. Petta, J. R. *et al.* Coherent manipulation of coupled electron spins in semiconductor quantum dots. *Science* **309,** 2180–2184 (2005).
7. Splettstoesser, J., Ol'khovskaya, S., Moskalets, M. & Büttiker, M. Electron counting with a two-particle emitter. *Phys. Rev. B* **78,** 205110 (2008).
8. Fève, G. *et al.* An on-demand coherent single-electron source. *Science* **316,** 1169–1172 (2007).
9. Field, M. *et al.* Measurements of Coulomb blockade with a noninvasive voltage probe. *Phys. Rev. Lett.* **70,** 1311–1314 (1993).
10. Ji, Y. *et al.* An electronic Mach–Zehnder interferometer. *Nature* **422,** 415–418 (2003).
11. Roulleau, P. *et al.* Direct measurement of the coherence length of edge states in the integer quantum Hall regime. *Phys. Rev. Lett.* **100,** 126802 (2008).
12. Talyanskii, V. I. *et al.* Single-electron transport in a one-dimensional channel by high-frequency surface acoustic waves. *Phys. Rev. B* **56,** 15180–-15184 (1997).
13. Koppens, F. H. L. *et al.* Driven coherent oscillations of a single electron spin in a quantum dot. *Nature* **442,** 766–771 (2006).
14. Bluhm, H. *et al.* Dephasing time of GaAs electron-spin qubits coupled to a nuclear bath exceeding 200 μs. *Nature Phys.* **7,** 109–111 (2011).
15. Buks, E., Schuster, R., Heiblum, M., Mahalu, D. & Umansky, V. Dephasing in electron interference by a 'which-path' detector. *Nature* **391,** 871–874 (1998).
16. Meunier, T. *et al.* Experimental signature of phonon-mediated spin relaxation in a two-electron quantum dot. *Phys. Rev. Lett.* **98,** 126601 (2007).
17. Barrett, M. D. *et al.* Deterministic quantum teleportation of atomic qubits. *Nature* **429,** 737–739 (2004).
18. Riebe, M. *et al.* Deterministic quantum teleportation with atoms. *Nature* **429,** 734–737 (2004).
19. Nielsen, M. A. & Chuang, I. L. *Quantum Computation and Quantum Information* (Cambridge Univ. Press, 2000).
20. Stevenson, R. M. *et al.* A semiconductor source of triggered entangled photon pairs. *Nature* **439,** 179–182 (2006).
21. Stotz, J. A. H., Hey, R., Santos, P. V. & Ploog, K. H. Coherent spin transport through dynamic quantum dots. *Nature Mater.* **4,** 585–588 (2005).
22. Gustavsson, S. *et al.* Counting statistics of single-electron transport in a quantum dot. *Phys. Rev. Lett.* **96,** 076605 (2006).
23. del Alamo, J. & Eugster, C. C. Quantum field-effect directional coupler. *Appl. Phys. Lett.* **56,** 78–80 (1990).
24. Tsukada, N., Wieck, A. D. & Ploog, K. Proposal of novel electron wave coupled devices. *Appl. Phys. Lett.* **56,** 2527–2529 (1990).

Supplementary Information is linked to the online version of the paper at www.nature.com/nature.

Acknowledgements We thank Y. Launay and P. Perrier for technical support. We acknowledge technical support from the 'Pôles Électroniques' of the 'Département Nano et MCBT' from the Institut Néel. M.Y. acknowledges financial support by Grant-in-Aid for Young Scientists A (no. 20684011) and ERATO-JST (080300000477). S.T. acknowledges financial support from Special Coordination Funds for Promoting Science and Technology (NanoQuine), Japan Science and Technology Agency Strategic International Cooperative Program, Japanese Ministry of Education, Culture, Sports, Science, and Technology KAKENHI 'Quantum Cybernetics', and Intelligence Advanced Research Projects Activity project 'Multi-Qubit Coherent Operations' through Harvard University. A.D.W. acknowledges expert help from D. Reuter and support of the Deutsche Forschungsgemeinschaft (SPP1285) and the Bundesministerium für Bildung und Forschung (QuaHLRep 01BQ1035). C.B. acknowledges financial support from Centre National de la Recherche Scientifique (DREI) – Japan Society for the Promotion of Science (nos PRC 424 and L08519). T.M. acknowledges financial support from Marie-Curie European Reintegration Grant 224786. We are grateful to the Nanoscience Foundation of Grenoble for partial financial support of this work.

Author Contributions S.H. and T.M. conceived and performed the experiments and analysed the data. Sh.T., M.Y. and S.T. were in charge of the sample fabrication and early stages of the experiment. A.D.W. performed the molecular beam epitaxy growth of the high-mobility GaAs/AlGaAs heterostructure. C.B and T.M. wrote the manuscript. All authors contributed to the manuscript and discussed the results extensively.

Author Information Reprints and permissions information is available at www.nature.com/reprints. The authors declare no competing financial interests. Readers are welcome to comment on the online version of this article at www.nature.com/nature. Correspondence and requests for materials should be addressed to C.B. (bauerle@grenoble.cnrs.fr) or T.M. (tristan.meunier@grenoble.cnrs.fr).